JOURNAL OF THE AMERICAN WATER RESOURCES ASSOCIATION

Vol. 51, No. 6 AMERICAN WATER RESOURCES ASSOCIATION December 2015

A GEOSPATIAL METHODOLOGY TO IDENTIFY LOCATIONS OF CONCENTRATED RUNOFF FROM AGRICULTURAL FIELDS[1]

Gregory Hancock, Stuart E. Hamilton, Monica Stone, Jim Kaste, and John Lovette[2]

ABSTRACT: A geospatial methodology has been developed that utilizes high resolution lidar-derived DEMs to help track runoff from agricultural fields and identify areas of potential concentrated flow through vegetated riparian areas in the Coastal Plain of Virginia. Points of concentrated flow are identified across 74 agricultural fields within the Virginia portion of the Chesapeake Bay watershed. On average, 70% of the surface area of the agricultural fields analyzed drains through less than 20 m of the field margin, and on average 81% of the field surface area drains through 1% or less of the field margin. Within the riparian buffer, locations that were predicted by the geospatial model to have high levels of concentrated flow were found to exhibit evidence of channelization. Results indicate that flow concentration and channelized flow through vegetated riparian areas may be common along the margin of agricultural fields, resulting in vegetated riparian areas that are less effective at sediment trapping than assumed. Additional results suggest that the regulations governing the location and width of vegetated riparian may not be sufficient to achieve goals for reducing sediment and nutrient runoff from nonpoint agricultural sources. Combined with the increasing availability of lidar-derived DEMs, the geospatial model presented has the potential to advance management practices aimed at reducing nonpoint source pollution leaving agricultural fields.

(KEY TERMS: agricultural runoff; GIS; lidar; Chesapeake Bay; riparian buffers.)

Hancock, Gregory, Stuart E. Hamilton, Monica Stone, Jim Kaste, and John Lovette, 2015. A Geospatial Methodology to Identify Locations of Concentrated Runoff from Agricultural Fields. *Journal of the American Water Resources Association* (JAWRA) 51(6):1613-1625. DOI: 10.1111/1752-1688.12345

INTRODUCTION

Agricultural lands occupy approximately 22% of the Chesapeake Bay watershed land area and account for 44% of the nitrogen, 44% of the phosphorous, and 65% of the sediment delivered to the Bay annually (USEPA, 2010). Agricultural practices such as fertilizer application, tilling croplands, and applying manure to agricultural fields are likely the primary origins of the sediment and nutrients (USEPA, 2010). Nutrient and sediment loads from agricultural runoff have increased over the last century (Kemp *et al.*, 2005), contributing to enhanced primary pro-

[1]Paper No. JAWRA-14-0192-P of the *Journal of the American Water Resources Association* (JAWRA). Received September 22, 2014; accepted May 20, 2015. **Discussions are open until six months from issue publication**.

[2]Professor (Hancock) and Associate Professor (Kaste), Department of Geology, College of William and Mary, Williamsburg, Virginia 23187; Assistant Professor (Hamilton), Geography and Geoscience, Salisbury University, 157Q Henson Science Hall, 1101 Camden Avenue, Salisbury, Maryland 21801; Graduate Student (Stone), Department of Geography, University of Alabama, Tuscaloosa, Alabama 35487; and Graduate Student (Lovette), Department of Geography, University of North Carolina at Chapel Hill, Chapel Hill, North Carolina 27599 (E-Mail/Hamilton: sehamilton@salisbury.edu).

ductivity and subsequent eutrophication in the Bay. Over the last several decades, the increased size and duration of anoxic zones within Bay waters (Officer *et al.*, 1984; Boesch *et al.*, 2001) have produced sharp declines in the population of aquatic species such as oysters, crabs, striped bass, and sturgeon. Such anoxic zones have not only impacted aquatic species but have also degraded the quality of water in the Bay that is used for human recreation and increased the occurrence of toxic algal blooms that are detrimental to human health (Kleinman *et al.*, 2011). In addition to the fauna impacts, suspended sediment exiting an agricultural field is likely partially responsible for the substantial reductions in sea grass coverage across the Bay (Kemp *et al.*, 2005).

The Chesapeake Bay watershed includes portions of Delaware, Maryland, New York, Pennsylvania, Virginia, and West Virginia as well as Washington D.C. In 1987, the states in the Chesapeake Bay watershed agreed to reduce controllable sources of nitrogen and phosphorous by 40% by the year 2000 in an effort to restore the Bay's health (Lowrance *et al.*, 1997; Boesch *et al.*, 2001) and this agreement became known as The Chesapeake Bay Agreement (CBA). The CBA mandated practices to decrease sediment and nutrient loads to the Bay in an effort to reduce the extent of subsequent eutrophication. As part of this effort, the Chesapeake Bay Protection Act (CBPA) requires the designation of Resource Protection Areas (RPAs) in a portion of the Bay's watershed on "lands adjacent to water bodies with perennial flow that have an intrinsic water quality value due to the ecological and biological processes they perform or are sensitive to impacts which may cause significant degradation to the quality of state waters" (Virginia General Assembly, 1989).

Within Virginia, RPAs are required in counties that have lands within the Coastal Plain portion of the Chesapeake Bay watershed. Lands adjacent to RPAs are required to have "a buffer area not less than 100 feet in width located adjacent to and landward of [RPAs], and along both sides of any water body with perennial flow" (Virginia General Assembly, 1989). These buffers are typically forested riparian areas, and are intended to capture sediment and uptake nutrients from surface runoff and subsurface flow before they enter adjacent water bodies draining to the Bay (Lowrance *et al.*, 1984, 1997) (Figure 1). Vegetative cover within the riparian buffer is assumed to slow the movement of overland flow, trap sediment, and increase runoff infiltration allowing for absorption of nutrients by vegetation (Lowrance *et al.*, 1986; Cooper *et al.*, 1987; Tomer *et al.*, 2009; Dosskey *et al.*, 2010). The CBPA states that buffers "shall be deemed to achieve 75% reduction in sediments and 40% reduction in nutrients" (Virginia General Assembly, 1989). These target reduction goals are based on measured reductions documented in studies of limited watersheds in the Chesapeake Bay region.

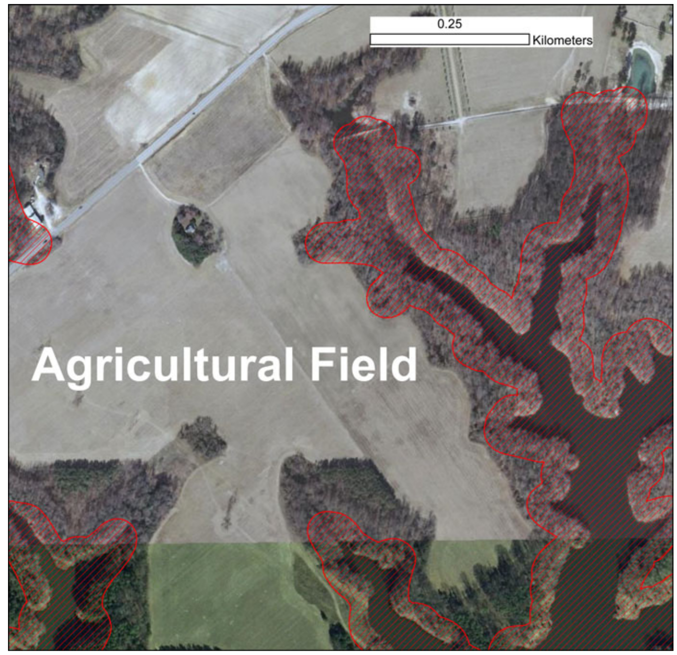

FIGURE 1. Legally Designated Riparian Buffers. The red hashes are a small section of the actual riparian buffer as legally delineated by James City County, Virginia. This section has a forested buffer bordering the agricultural field and perennial body of water. The agricultural field drains into the buffer and then on into the perennial body of water.

Forested riparian areas have been shown to be effective at reducing nutrient and sediment loads in runoff from agricultural fields. Within the Coastal Plain, it has been stated that forested riparian buffers may accomplish sediment, nitrogen, and phosphorous reductions of approximately 96, 75, and 77%, respectively (Lowrance *et al.*, 1997). Measured reductions of total nitrogen and phosphorous by riparian buffers range from 67 to 89% and 24 to 81%, respectively (Peterjohn and Correll, 1984; Lowrance *et al.*, 1986).

Existing Coastal Plain studies have focused primarily on nutrient and sediment reduction in groundwater rather than surface flow, and the estimates of nutrient and sediment reduction cited above assume that concentrated and channelized surface flow within the buffers does not occur (Lowrance *et al.*, 1997). Optimal performance of forested riparian buffers requires that overland flow be distributed across as much of the riparian buffer as possible (Dillaha *et al.*, 1989; Dosskey *et al.*, 2002; Knight *et al.*, 2010). However, concentrated flow may be a common occurrence on agricultural fields, generated by natural field topography, furrow orientation, surface topography modifications, ditching, and road surfaces (Dosskey *et al.*, 2002; Blanco-Canqui *et al.*, 2004; Verstraeten *et al.*, 2006; Knight *et al.*, 2010; Pankau *et al.*, 2011; Hösl *et al.*, 2012). Numerous studies have suggested that flow concentration reduces the efficiency of pollutant and sediment removal by buffers (Dillaha *et al.*, 1989; Daniels and Gilliam, 1996; Dosskey *et al.*, 2002; Helmers *et al.*, 2005; Mayer *et al.*, 2007; Fox *et al.*, 2010; Knight *et al.*, 2010), in part because flow concentration may substantially increase the contributing area-to-buffer area ratio, thus reducing the buffer area actively utilized for nutrient and sediment trapping (Dosskey *et al.*, 2002).

In Nebraska, it was found that flow concentration reduced the effective buffer area on four agricultural fields to between 6 and 81% of the gross buffer area and this increased the contributing area to effective buffer area ratio to between 30:1 and 100:1 (Dosskey *et al.*, 2002). Additionally, 27 to 71% of the buffer area was also drained by gullies feeding directly into receiving streams (Dosskey *et al.*, 2002). Modeling of sediment trapping on these fields suggests that flow concentration reduces the sediment trapping efficiency of buffers by 7 to 56% compared to the assumption of widely distributed flow (Dosskey *et al.*, 2002). The reduction in sediment trapping efficiency would likely reduce total phosphorous trapping, as much of the phosphorus in runoff is sediment bound (Dillaha, 1987; Abu-Zreig *et al.*, 2003). Concentrated flow may also promote channel incision and expansion within forested buffers, allowing water to effectively bypass buffers with little to no trapping of sediments or absorption of nutrients (Dosskey *et al.*, 2002; Knight *et al.*, 2010).

Despite the implementation of the CBPA, reduction in nonpoint sources of sediment and nutrients, such as agricultural runoff, has lagged behind that of point source reduction, and the goal for 40% reduction had not been met as of 2011 (National Research Council, 2011). Data collected by the Chesapeake Bay Program indicate that nitrogen, phosphorus, and sediment delivered to the Bay in 2012 was approximately 20, 40, and 60% lower, respectively, than the average load delivered between 1990 and 2012 (Chesapeake Bay Program, 2014). In 2011, however, the nitrogen, phosphorus, and sediment loads delivered to the Bay were approximately 40, 200, and 400% higher, respectively, than average, and there is no declining trend in loads delivered to the Bay over the period of measurement (Chesapeake Bay Program, 2014).

Widespread occurrence of flow concentration on agricultural fields could potentially reduce the effectiveness of vegetated riparian areas within the Chesapeake Bay watershed, resulting in less trapping of sediment and nutrients than assumed. If true, extensive buffer-bypassing by flow concentration could be partly responsible for the failure to meet the CBPA goals for nutrient and sediment load reduction. However, a methodology for rapidly quantifying the extent of concentrated flow has not been readily available, and hence a systematic evaluation of the frequency and distribution of concentrated flow within the Chesapeake Bay watershed has not been completed and thus warrants study.

This article presents a detailed geospatial methodology for evaluation of the potential for flow concentration at the margins of agricultural fields using readily available topographic data and imagery. This methodology builds on previous Geographic Information Systems (GIS)-based precision conservation strategies (Tomer *et al.*, 2003, 2009; Burkart *et al.*, 2004; Dosskey *et al.*, 2005, 2011) and provides a rigorous methodology for assessing flow concentration at agricultural field margins and the buffer area to contributing area ratio of agricultural field-scale watersheds. However, the GIS method presented here differs from the previously published strategies in several significant ways. First, the model is constructed to use lidar-derived geospatial data with substantially greater resolution (~3 m cell spacing), which has become much more widely available in the last several years. The previous efforts relied on elevation data derived from topographic map interpolation with a resolution of 10 to 30 m spacing. Second, our method focuses on identifying flow concentration and buffer bypassing in existing forested buffers required by regulation, and the method is applied across the Virginia Coastal Plain portion of the Chesapeake Bay watershed where forested buffers are required by law. In contrast, previous strategies were developed with the goal of identifying streamside locations where buffers could be placed for maximum benefit (e.g., Tomer *et al.*, 2003, 2009). The ability to identify deficiencies in existing forested riparian buffer effectiveness could steer corrective actions to those locations where such actions would be most beneficial. Third, the model codes and explicit instructions for using them are provided to allow rapid and cost-efficient implementation of this strategy by regulators, researchers, and planners. Finally, we have examples taken from the Virginia Coastal Plain portion of the Chesapeake Bay watershed, where our initial data and observations show that substantial flow concentration on agricultural fields is common and is well-identified by our strategy.

Study Area

In Virginia, the 46 counties and cities located in the Coastal Plain region of Virginia fall under the jurisdiction of the Chesapeake Bay Act of 1988 (Vir-

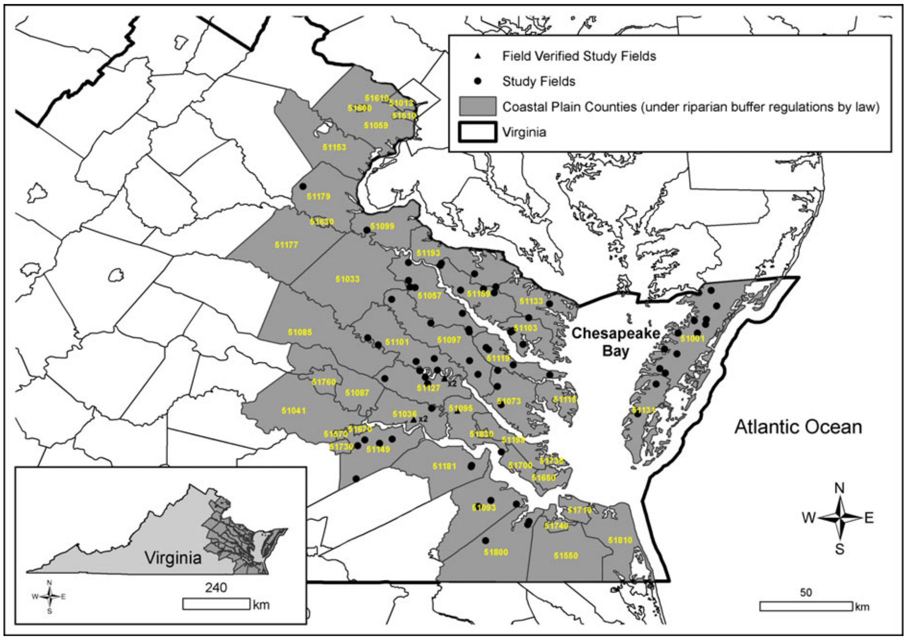

FIGURE 2. Study Area. Study sites are represented with black dots or black triangles if they are field verified. Counties under the riparian buffer regulation are filled in dark gray with the FIPS code listed. No study sites exist in the western region due to a lack of suitable lidar coverage.

ginia General Assembly, 1989) (Figure 2). All agricultural fields within these counties and cities are therefore covered under the RPA requirement of the Chesapeake Bay Act, and hence require riparian buffers adjacent to perennial streams and tidal wetlands (Virginia General Assembly, 1989). For this study, agricultural fields were randomly selected from that portion of the Virginia Coastal Plain area in which lidar data are available with sufficient point spacing to create field-level terrain models. Lidar data are available for approximately 88% of the total area that falls under the Chesapeake Bay Act in the Virginia Coastal Plain.

Lidar-Based Digital Terrain Models

An impediment to mapping flow direction and concentration at the level of a single agricultural field level has been the historic lack of high-resolution (e.g., point spacing of <2 m) terrain data capable of resolving micro-drainage patterns over a large area. To determine how widespread flow concentration might be on agricultural fields over a region, such data must also be available over large geographic areas to obtain a representative sample of agricultural fields. Elevation products that cover large geographic areas such as the 1 arc-second or 1/3 arc-second USGS National Elevation Database (NED) models are unlikely to provide a sufficient number of terrain points within a particular agricultural field to reasonably depict sub-field drainage patterns. On the other hand, high-resolution surveys are typically achieved by utilizing tripod mounted traditional laser survey equipment or more recently by portable laser scanners and highly accurate GPS systems, which are rarely available for entire regions. In addition to the geographic extent issues, traditional field survey methods require physical access to a property for a substantial period of time with at least two people. Hence, even if agricultural field access can be achieved it is prohibitively expensive in terms of time, equipment, and labor to survey many hundreds of fields containing many millions of elevation points. Therefore, the required data for such analysis are either available over large areas but with insufficient resolution (e.g., NED, Shuttle Radar Terrain Models, ASTER DEM), or the data have sufficient resolution but have limited geographic extent precluding unbiased sampling (Tripod laser surveys, Differential GPS surveys). Photogrammetric and stereo GIS techniques do exist for creating high-resolution digital terrain models (DTMs) over large geographic areas, but both of these methods are again time consuming, expensive, and require supplemental data, such as reliable ground control solutions for extraction of terrain.

Where available, airborne lidar data can provide adequate resolution and sufficient geographic coverage to assess runoff pathways from agricultural fields. The point spacing of lidar is often greater than one point per two meters squared, allowing for extraction of finely detailed flow pathways and drainage patterns based on at least several thousand accurate x, y, z coordinates contained within a typical field boundary. In the study area, lidar data also overcomes the geographic extent impediment listed above, as it is usually flown at the county or regional level. Most of the lidar data for this analysis were flown at the regional level as part of the Federal Emergency Management Agency (FEMA) Flood Mapping Program. One additional benefit of lidar data generated as part of the FEMA Flood Mapping Program is that it meets predefined accuracy standards based on independent ground control and quality assurance of the data. Thus, accurate error statistics and confidence levels about lidar elevation readings are reported with the basic lidar point data. In addition, mapping of field drainage using lidar-derived DTMs does not require physical access to the agricultural field, thus eliminating the time and cost associated with obtaining permission for on-site work and field surveying of many agricultural fields. With a large lidar dataset, study locations can be chosen randomly, without the limitation on field selection imposed by the need for access permission.

METHODS

Field Selection

Study fields are randomly selected using the following procedure. Within the study area (Figure 2), the 30 m resolution 2006 National Land Cover Database (NLCD) was queried to return all cells with a cultivated crops classification. This resulted in 2,182,052 cultivated crops cells with a total area of 1,964 km^2. Each of the cells was assigned a unique value between 1 and 2,182,052. The Python library random number generator was used to produce a number between 1 and 2,182,052 and the field containing the randomly selected cell with that number was then accepted or rejected as a study site based on the five criteria below.

A cell was rejected if it met any of the following criteria: had been previously selected at random, was within 1 km of a previously selected cell, was not located in a known agricultural area, was not within 1 km of a perennial stream, or drained directly into tidal waters rather than perennial streams. Agricultural status of a cell was confirmed by visual inspection of color aerial photography collected in 2006/2007 (i.e., when the NLCD was completed) and in 2011 (i.e., when the lidar data was collected) and/or field verification.

The process above was repeated iteratively until 70 random cells, and the agricultural fields containing them, had been accepted. One of these fields was later rejected due to errors in the lidar data. In addition to the 69 randomly generated fields, 5 nonrandom fields were added to the analysis. Within these 5 additional fields, permission had been obtained to complete field studies comparing the GIS-based flow predictions to evidence for flow on those agricultural fields. Thus, a total of 74 fields were analyzed, all of which should be required to maintain vegetated riparian areas around some portion of the field according to the guidelines in the CBPA.

Field DTM Creation

Lidar data collected between 2010 and 2011 in early spring leaf-off conditions flown by two commercial vendors was utilized as the base product for all analysis. Both vendors used the Optech ALTM 3100EA lidar system (Optech Inc., Vaughan, Ontario, Canada). Point densities varied from one point per 0.5 m^2 to one point per 0.7 m^2. From the three-dimensional multi-return lidar data cloud, ground points were extracted by the vendors using a proprietary Terrascan algorithm combined with human-based three-dimensional visualization techniques. This combined with stereo-derived breakline features allowed for the creation of accurate DTMs. As lidar terrain models are actually interpolated, the final DEM relies on the accurate delineation of the breakline features to better represent the surface topography. Breaklines are typically lines that divide drainage areas such as the tops of ridges, streams, or other important linear features. Stereo processing is the use of stereo imagery and photogrammetric methods to obtain accurate breaklines.

All DTMs were delivered with horizontal coordinates in the Virginia State Plane South (NAD 1983, NSRS2007 adjustment) coordinate system with the linear unit of US survey feet. The vertical coordinate system in the original DTM data is NAVD 1988 with vertical units in feet and tenths. The horizontal coordinates were projected to UTM Zone 18N (NAD 1983) accounting for the NSRS2007 adjustment with a horizontal unit of meters, and the vertical coordinate system of NAVD 1988 was preserved but converted to meters. Field verification of point data by the vendor resulted in the root mean square error varying across the study between a low of 0.09 m to a high of 0.22 m at the 95% confidence level. The lidar data was resampled to obtain a 3-meter grid spacing for the field level DTMs.

Portions of the raster DTM were extracted to include each selected agricultural field, including a

2 km buffer around each field, from the random cell used to select the field. The buffer allowed space to capture the upstream drainage area and the resulting accumulated flow entering the agricultural field. The field-specific DTMs were then preprocessed, using the D8 algorithm to fill sinks within the DTM followed by the generation of a flow direction raster (Jenson and Domingue, 1988). The flow direction grid was then processed into a flow accumulation raster, with each cell value representing the number of cells upstream, allowing for the calculation of the accumulated flow above each cell. The flow accumulation is defined as the cumulative contributing drainage area for each observed location.

Watershed Determination

Following calculation of accumulated flow, the edge of the active agricultural field (i.e., the field margin) was manually digitized using heads-up digitizing from 1 m resolution aerial imagery flown in 2008. The field margin is defined as the boundary between the actively maintained agricultural field and adjacent land not used for farming, typically woodlands. While being digitized, field margin points were snapped to the center of the nearest cell in the accumulated flow raster. In deciding where to place points on the field margin, a four cardinal direction digitizing strategy was utilized to standardize the procedure and minimize the possibility of missing cells of substantial accumulated flow that cross the field margin (Figure 3). In locations where flow directions were parallel to the edge of fields, the digitized field margin was moved a few cells in either direction to prevent double-counting of accumulated flow (Figure 3). Following the manual creation of the field margin, the flow direction and flow accumulation rasters are sampled at each cell along the field margin. This yields the direction of flow at each field margin cell (e.g., on, parallel to, or off the field) and the cumulative number of cells upstream of each field margin cell. The accumulated flow was determined by multiplying the number of cells upstream of each field margin cell by 9 m^2 (i.e., the 3×3 m area represented by each cell).

A 3 m DEM cell resolution was selected primarily due to compatibility with 1/9 arc-second NED DEMs that are currently available for approximately one-third of the United States (U.S.) with substantial increases in coverages planned for the near future (USGS, 2014). In addition to 3 m, both 10 and 1 m DEMs were tested for suitability. The 10 m DEMs would have allowed for almost total national compatibility with current NED products but 10 m resolution DEMs proved too coarse on smaller fields to accurately capture micro-drainage field level features that are clearly visible in the lidar data. On the other hand, 1 m DEMs captured such features but required substantially longer processing times, approximately three times longer to delineate each field boundary, and resulted in data approximately nine times the size without any significant improvement in depicting field level drainage patterns. Additionally, a model tuned for 1 m data would have only been applicable to a very limited portion of the continental U.S. with the lidar data available to build extremely high resolution DEMs and would require the user to have access to the software, skills, and data to process their own lidar data. Users of the model may be able to utilize 10 m data in regions with high slope metrics and relatively large field areas. Conversely, it is possible that regions with small fields in areas with limited slope may require higher resolution DEMs.

This analysis is only concerned with areas generating flow from within, and exiting from, agricultural fields. In many cases, a portion of the upstream

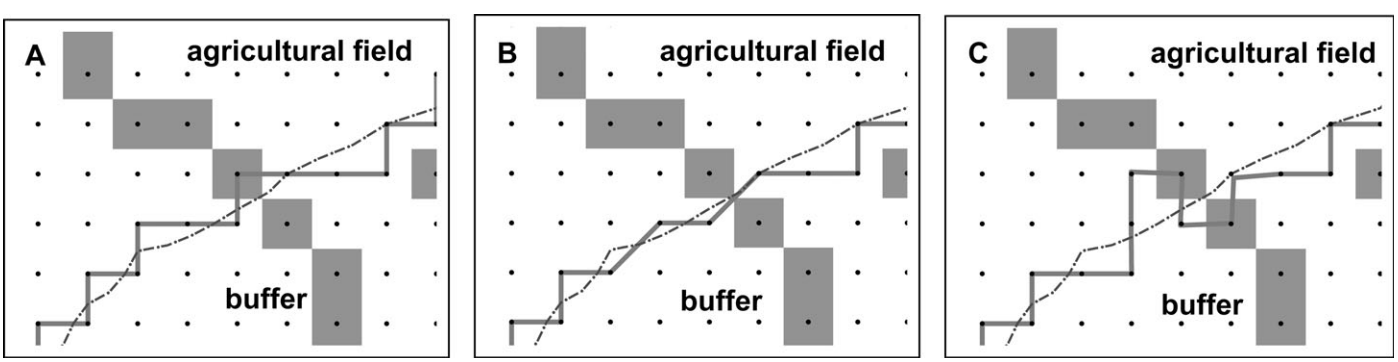

FIGURE 3. Accumulated Flow Crossing a Field Margin. The dotted line represents the field margin. The solid line represents the digitized field margin. The solid gray boxes represent the flow accumulation raster data flowing from the field in the north into a riparian buffer in the south. The black dots represent the accumulated flow data in vector point format. In panel (A) the 4-neighbor digitization catches the accumulated flow in one location only. In a 4-neighbor digitizing system all accumulated flow is captured, it is not possible to miss off field flow. Panel (B) represents an 8-neighbor digitization process. Note that it is possible to omit flow in the 8-neighbor system so this system was not utilized. Panel (C) shows the possible duplication of flow capture in the 4-neighborhood system. Data was checked for this inconsistency.

drainage area at a field margin point, where flow exits the field, is outside of the agricultural field. To remove off-field accumulated flow contribution from the total accumulation area, the ten points along the digitized field margin with the greatest total off-field directed accumulated flow were used as pour points to delineate the watershed above each point. The portion of each watershed solely within the digitized agricultural field margin was obtained by clipping the watershed to the interior extent of the digitized field margin. The area of each clipped watershed was calculated to determine the value of the accumulation area derived solely from the agricultural field for each of the ten watersheds. These watersheds were then re-ranked based on their field-derived accumulation area. The ten points with greatest accumulated flow accounted for, on average 81% of the total accumulation area crossing the field margin on the selected fields. Hence, ten points were sufficient to capture a large fraction of the total accumulation area on the field. As the digitized field margin polygons typically contain thousands of boundary points, the procedure was limited to the largest ten watersheds on each field. The ten largest watersheds represent almost all the flow variation, therefore it would be impractical and unnecessary to construct watersheds for each point on the field margin.

Model Compilation

ArcGIS model builder was utilized to create an automated model, Identifying Points of Concentrated Flow on Agricultural Fields (IPCFAF), from which fields can be analyzed using DTMs as outlined in the above methodology. This model was created to ensure consistency in field analysis regardless of location or user, and to improve efficiency in the completion of multiple-field analyses. The model requires two users inputs (a DEM raster and a field outline), contains 78 distinct steps, and produces 16 output files providing data on point elevation, flow direction and accumulated flow for all points, and accumulated flow at field margins derived solely from the fields. The model is provided as a supplement submission.

Using the DTM raster of the field, Part 1 of the model analyzes the DTM to determine accumulated flow, flow direction, and slope at each point within the DTM. The output is used to then create the field margin using the heads-up digitization method discussed above. Using digitized field margin, Part 2 of the model extracts watersheds for the ten points of greatest accumulated flow, and clips them to contain only accumulation area originating from the field. The automated steps of the model ran in less than one minute on a standard PC (2.4 GHz Intel processor, 2 GB RAM), and the GIS users digitized an average of four fields in an hour. The output files for the 74 fields included in this analysis occupy approximately 9 GB of compressed spatial storage space.

Comparison of GIS Analysis to Observations of Flow

The GIS analysis provides a measure of upstream accumulation area at each point along a digitized field margin, allowing a prediction of where runoff might be concentrated. Obviously, this strategy does not quantify actual flow at the field margin points. To ground-truth the GIS-based methodology to predict locations of high accumulated flow, field surveys were completed on five of the agricultural fields analyzed using the methods described above. Field surveys were limited to agricultural fields where access was allowed by the landowner; therefore, unlike the rest of the analyzed fields, these were not randomly chosen. At each of the five fields, evidence for concentrated flow moving across the field margin was noted by walking along the well-defined edge of the cultivated field. Field evidence of concentrated flow included deposits of water-transported sediment and organic materials (e.g., sticks, leaves), flattened plants oriented in a common direction, and ephemeral and permanent channels extending directly off the field into adjacent lands (Figure 4). Where evidence of surface flow was observed, it was noted whether it was dispersed (e.g., overland flow) or confined within channels. Observations of evidence for flow were ranked on a four-point scale: 1 = evidence of water movement and overland flow, 2 = similar to 1 but evidence for movement of debris and a concentrated flow, 3 = small continuous or discontinuous channel (<0.5 m in width), and 4 = large, continuous channel (>0.5 m in width). Where filed evidence for concentrated flow existed, a Trimble GeoXT GPS unit connected to a Trimble Hurricane antenna (Trimble Navigation Limited, Sunnyvale, California) was utilized to obtain the location of the flow. GPS point locations were differentially corrected in Trimble Pathfinder Office V5.1 using base stations within 25 km of the surveyed field, providing sub-meter GPS resolution.

To determine if flow actually occurred at locations of high accumulated flow predicted by the GIS methodology, temporary stream gaging station was installed in an ephemeral channel draining one of the study fields (Caverly *et al.*, 2013). The well-defined channel began at the field margin, with an upstream drainage area of 0.21 ha (52 acres), all of which was on cultivated land (Figure 5). The gaging station measured water height in the channel ~25 m downstream of the field margin. Whenever flows exceeded ~6 cm depth, water surface elevation was recorded

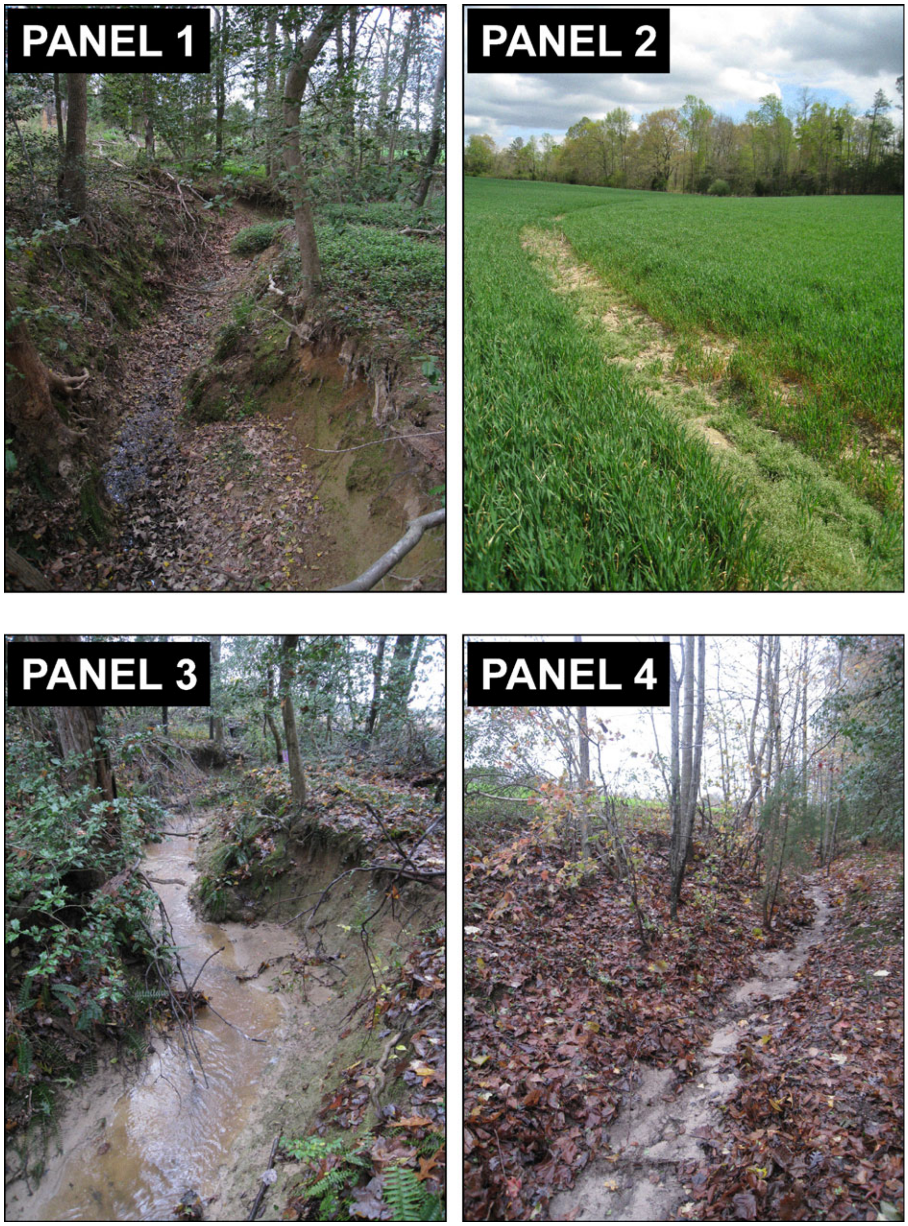

FIGURE 4. Overland Flow as Seen in the Field. Examples of evidence of field margin flows that align with the modeled data. All images are in or entering a riparian buffer. Panel 1 and Panel 3 represent large continuous channels downstream of a field. Panel 2 represents flattened material and debris on a field. Panel 4 represents transported sediment and deposited material slightly downstream of a field margin.

every five minutes. Discharge in the channel was measured on four separate occasions using salt dilution gaging method (Day, 1976). The measured discharge values were coupled with a survey of the channel cross section to determine a value for the roughness coefficient in the Mannings velocity equation. This calibration coupled with the survey of channel cross section and slope enabled prediction of discharge at any water depth in the channel, allowing us to calculate discharge from the water surface elevation data collected by the automated gaging station. In addition, a tipping bucket rain gage with a precision of 0.01" was installed within the gaged watershed. The gaging station and rain gage were in operation between June 9, 2010 and October 22, 2010 and between March 18, 2011 and September 15, 2011.

RESULTS

As a demonstration of the data that can be produced using this model, the initial analyses of the 74 agricultural fields in the Coastal Plain portion of the

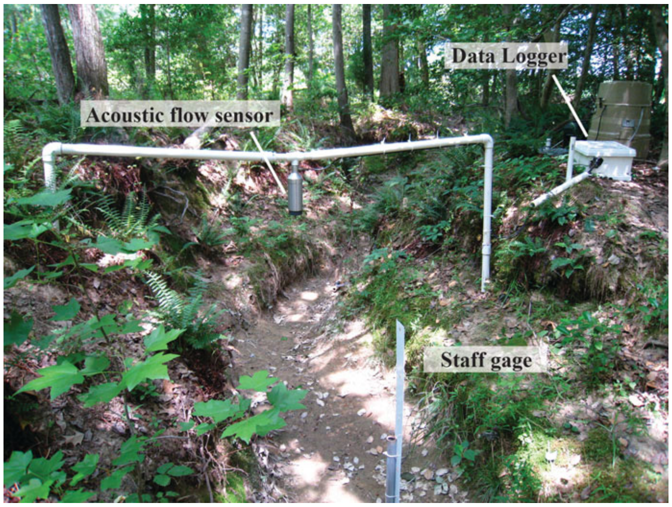

FIGURE 5. Field Flow Verification. Flow gaging station in an ephemeral channel with the entire upstream area containing cultivated land on one of the analyzed fields. Water level is measured by an acoustic flow sensor every minute during flow events.

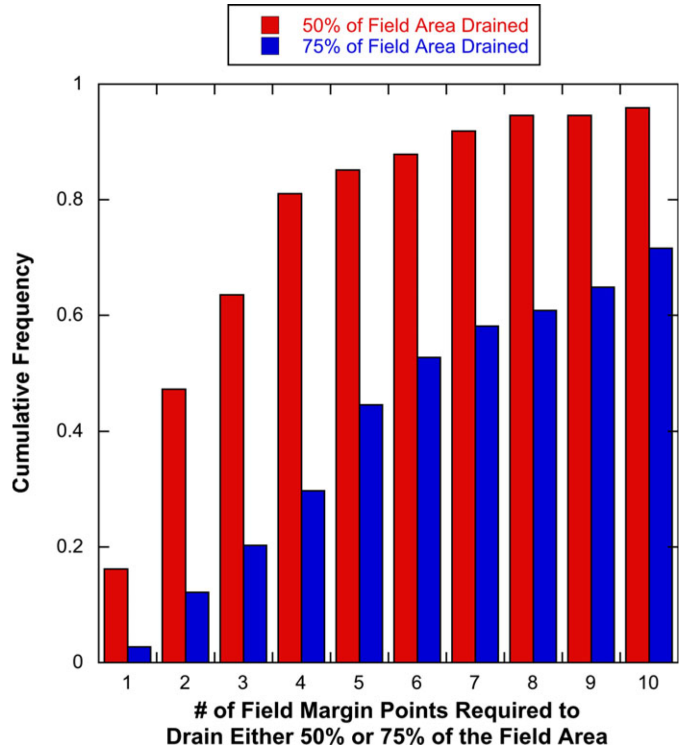

FIGURE 6. Field Margin Drainage Statistics. This figure depicts the number of field margin points that drain either 50% of an entire field or 75% of an entire field.

Chesapeake Bay watershed in Virginia are presented. The size of the randomly selected agricultural fields ranged from 0.1 to 0.71 km^2, with an average field margin length of 3.1 km. The combined area of all fields is 14 km^2 and the combined field margin length is 226 km. A 3 m cell size was used to create the DTMs in this study, thus a total of 1,500,176 cells classified as agricultural land by the NLCD were analyzed. The total number of field margin points was 75,420.

Accumulated Flow at Field Margins

The field margin point predicted to have the greatest accumulated flow on each field captured 8 to 83% of the total accumulation area on the field, with an average of 34% for all fields. The five points with greatest accumulated flow on the digitized field margin drained between 29 and 100% (average = 70%) of field area, and the comparable ten points with greatest accumulated flow drained between 41 and 100% (average = 81%) of field area. The ten points on the field margin with greatest accumulated flow (total of 740 points across all fields) represent only ~1% of all the points digitized on the field margins, and hence only ~1% of the total field margin length, while draining ~81% of the combined field area. For 63 of the 74 fields, 50% of the field drained through five points or less along the digitized field margin, and on 36 of the fields 50% of the area drained through only one or two points (Figure 6). Further, for 33 of the 74 fields, 75% of the field drained through five or fewer points along the field margin, and 9 of these required only two or less points to drain 75% of the field (Figure 6).

These results indicate that a large proportion of each agricultural field analyzed is being drained through a small proportion of the field margin. For example, the number 2 on the x axis — red bar — means that on average almost 50% of the fields drain 50% of their total area through only two points on the field margin then on into the riparian buffer. That is, 50% of any given field drains through only 6 m of the average margin of 3.1 km. The number 6 on the x axis — blue bar — means that on average almost 50% of the fields drain 75% of their total area through only six points along the field margin and then on into the riparian buffer. That is, 75% of any given field drains through only 18 m of the average margin of 3.1 km. These example results illustrate the utility of the procedure for assessing flow concentration on agricultural fields, and suggest flow concentration is common in the Coastal Plain study area.

Validation of Concentrated Flow on the Fields

Within Figure 7, each panel presents results from the five agricultural fields that were physically accessed and analyzed for evidence of overland flow.

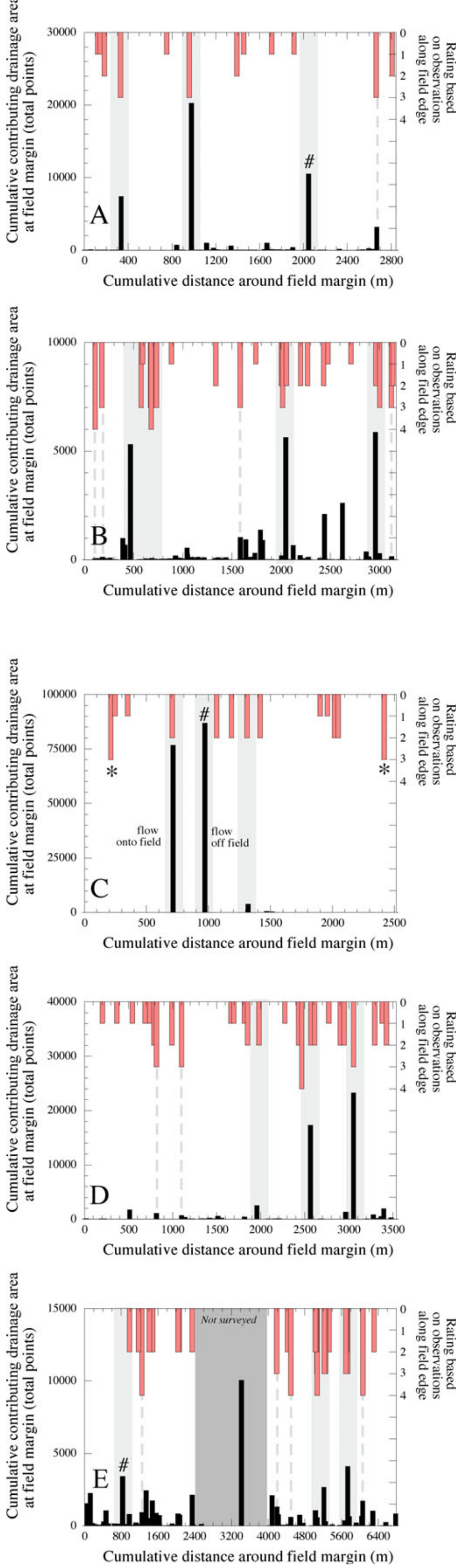

FIGURE 7. Comparison of Observed Evidence for Surface Flow to the Accumulated Flow at the Field Margin Obtained from the GIS Analysis. The x-axis represents the distance around the field margin. The lower y-axis represents the cumulative contributing drainage area at each location on the x-axis. The upper y-axis represents the evidence of surface flow from field observations for each point on the x-axis.

The red bars (right y axis) show the flow evidence ratings observed along the field margin. Black bars (left y axis) show accumulated flow (e.g., total number of pixels draining to each point) along the digitized field margin. The three field margin points with greatest accumulated flow are shaded in gray. The number symbol (#) identifies field margin points with high accumulated flow, but no observed evidence of flow on the field. Note that only 3 of the 15 points with greatest accumulated flow cannot be directly linked to evidence of flow observed in the fields. Dashed gray lines connect field margin points with evidence of channelized surface flow (rating of 3 or 4) to accumulated flow predicted for that point, while the asterisk symbol (*) identifies field margin points with observed evidence for flow on the field but no accumulated flow as predicted by the GIS analysis. Note that only 2 of the 23 points with evidence for channelized flow (rating of 3 or 4) could not be linked to points predicted to have accumulated flow in the GIS analysis.

In Figure 7, the location of cells with the highest accumulated flow along the field margins obtained from GIS are compared to the locations where evidence of flow was observed. In each figure, the three locations along the field margin with the greatest accumulated flow are highlighted and are compared to the ranking of evidence for flow based on field observations at the same location. Of the 15 points (three points from five fields) highlighted in each panel of Figure 7, 12 (80%) can be directly matched to points with field evidence of flow observed at nearly the same position at the field margin. Of the 15 points, 9 (60%) are predicted at nearly the same position as channels observed at the field margin (Figure 7). Of the 23 points on field margins where channels were observed (ranking of 3 or 4) on the five fields, 21 can be straightforwardly matched with points on the field margin where the GIS analysis predicts at least some flow concentration at the field margin. This not a statistically robust test of the validity of the GIS technique; however, a strong agreement was observed between the GIS-based predictions of the locations of flow concentration and the field observations of evidence for flow concentration. This agreement occurred despite the ephemeral nature of runoff generation on the fields; destruction of evidence for overland flow and channelization by surface disturbance during plowing, grading, and fertilizer and herbicide application on the field in between rainfall events; poor visibility of flow evidence beneath dense crop and forest cover; and short-term access to the fields. Hence, evidence for flow may simply have been erased since the last event in places along the field margin with low flow frequency or may have been missed in locations of dense vegetation.

During the period, the gaging station was operating on one field, six flow events were recorded at the gaging station location. The total precipitation generating these flows ranged from 2.1 to 21.4 cm, with corresponding recurrence intervals from less than one year to fifty years based on regional intensity-duration-frequency curves. Of the six flow events, three were generated by storms with recurrence intervals of one year or less, indicating that the generation of concentrated flow at this location likely occurs several times a year on average. These data provide direct evidence that concentrated flow may occur frequently in at least one field margin location where the GIS method identified high accumulated flow. On a subset of the field sample, it was determined that the export of organic carbon off the field during these periodic flow events equals or exceeds estimates of annual exports from forested catchments, indicating that these periodic flows are potentially important sources for nutrient delivery from agricultural lands (Caverly *et al.*, 2013). The export of sediment, nitrogen, and phosphorus during these flow events will be the subject of a separate manuscript.

CONCLUSIONS

The geospatial methodology developed is an effective way to determine areas of flow concentration at the level of individual agricultural fields. The 3 m lidar-derived DEMs were of sufficient resolution to determine accurate flow accumulation patterns across the agricultural fields analyzed in the study area. The potential for highly concentrated flow was observed on all 74 fields analyzed in the portion of the Virginia Coastal Plain studied. Most notable is the finding that 41 to 100% of these fields were drained through just ten points along the field margin (typically <0.2% of the total margin points on each field) (Figure 6). The points along the GIS-derived field margins that possessed the high accumulated flow values generally correspond with evidence of concentrated and channelized flow observed on the five fields surveyed for evidence of flow.

The methodology presented is compatible with 3 m DEMs generated from lidar data as currently utilized in the NED and is available for much of coastal Virginia and coastal Maryland. As the USGS continues to expand access to lidar-derived 1/9 arc-second (3 m) DEMs, the methodology and model presented can be utilized to systematically assess areas with potential for concentrated flow exiting agricultural fields. Such a process allows for local, regional, and eventually even national evaluation of concentrated flow as opposed to the current method of *in situ* surveys that are costly, time-consuming, and require property owner approval to access each field. Complete regional assessments allow for precise targeting of management practices at the field level as opposed to countywide regulations regardless of the need for the practice at each location. For example, riparian buffers could be optimally designed for each field in a county to maximize the efficiency of the buffers as opposed to applying a single uniform buffer that is likely ineffective in areas of high concentrated flow and unnecessary in areas of little or no potential flow.

Utilizing the model, it is shown that on average the majority of accumulated flow exits an agricultural field at less than 0.5% of the respective field boundary. Expanding the riparian area around these few exit points while decreasing the riparian area where no flow exits a field may provide the dual benefits of increasing the effectiveness of the riparian buffers while substantially increasing the potential land under crop. Indeed, many fields have the majority of their potential flow exiting in only one channel and these fields may be candidates for engineering solutions that capture sediment at the field margin although such solutions require further research.

While the GIS methodology presented here focuses on surface water flow pathways, this method is ultimately a technique to identify buffer locations that may be ineffective at trapping sediment and nutrients delivered from agricultural fields. The removal of nitrogen, phosphorus, and sediment by riparian buffers is most effectively accomplished when water moves through buffers as groundwater or widely disseminated (e.g., unconcentrated) sheet flow (e.g., Lowrance *et al.*, 1997). As discussed earlier in this article, concentrated and channelized flow through buffers dramatically decreases the nutrient and sediment retention by buffers (Dillaha *et al.*, 1989; Daniels and Gilliam, 1996; Dosskey *et al.*, 2002; Helmers *et al.*, 2005; Mayer *et al.*, 2007; Fox *et al.*, 2010; Knight *et al.*, 2010). Hence, the methodology to remotely identify specific field locations of buffer bypassing could facilitate the mitigation of previously unidentified sources of pollution to streams adjacent to agricultural fields.

In the case study presented here, the GIS analysis predicts that all of the fields evaluated in the Virginia Coastal Plain have points of highly concentrated flow accumulation, and visual surveys of five fields and flow monitoring on one field confirm that concentrated, channelized flow occurs at the points predicted by the GIS analysis. Widespread buffer bypassing by flow concentration at field margins, previously unrecognized in the study region, may be a significant additional source of nutrients and sediment to the Chesapeake Bay. Although this study is restricted to the Virginia Coastal Plain, it is likely that buffers in other portions of the Chesapeake Bay watershed have similar runoff characteristics. This unrecognized and potentially widespread occurrence of concentrated and channelized flow at field margins may be in part responsible for the slow pace of sediment and nutrient reduction in the Bay despite the remedial efforts initiated by the 1987 CBA.

SUPPORTING INFORMATION

Additional Supporting Information may be found in the online version of this article:

(1) A supplemental methods document provides additional GIS detail with diagrams for most of the key steps of the process. The supplemental methods document also includes a schematic model of the method. (2) A toolbox for ArcGIS 10.1 that includes the models utilized to calculate the field margin flow in this analysis. Researchers may utilize or modify these models in their own research while citing this article as the source. (3) A complete user manual with screen captures is enclosed and provides a step-by-step breakdown to assist in implementing the model.

ACKNOWLEDGMENTS

Thank you to Sarah Byrd for assistance digitizing the fields, tuning the model, and supervising students working on this project. Thanks to students of GEOL 440 (William and Mary) for help developing the data and digitizing fields. As always, we appreciate the Virginia Geographic Information Network for making available the lidar source files and FEMA for funding the original lidar flights. Thank you to the farmers and landowners who allowed us onto their property to conduct field work. Thank you to David Loss, Sarah Young, and Lyndsey Funkhouser for earlier iterations of this research. Thank you to the Virginia Environmental Endowment and the Charles Center (William and Mary) for funding portions of this research.

LITERATURE CITED

Abu-Zreig, M., R.P. Rudra, H.R. Whiteley, M.N. Lalonde, and N.K. Kaushik, 2003. Phosphorus Removal in Vegetated Filter Strips. Journal of Environmental Quality 32:613-618, doi: 10.2134/jeq2003.6130.

Blanco-Canqui, H., C.J. Gantzer, S.H. Anderson, and E.E. Alberts, 2004. Grass Barriers for Reduced Concentrated Flow Induced Soil and Nutrient Loss. Soil Science Society of America Journal 68:1963-1972, doi: 10.2136/sssaj2004.1963.

Boesch, D.F., R.B. Brinsfield, and R.E. Magnien, 2001. Chesapeake Bay Eutrophication. Journal of Environmental Quality 30:303-319, doi: 10.2134/jeq2001.302303x.

Burkart, M.R., O.E. James, and M.D. Tomer, 2004. Hydrologic and Terrain Variables to Aid Strategic Location of Riparian Buffers. Journal of Soil and Water Conservation 59:216-223.

Caverly, E., J.M. Kaste, G.S. Hancock, and R.M. Chambers, 2013. Dissolved and Particulate Organic Carbon Fluxes from an Agricultural Watershed during Consecutive Tropical Storms. Geophysical Research Letters 40:5147-5152, doi: 10.1002/grl.50982.

Chesapeake Bay Program, 2014. Track Our Progress. http://www.chesapeakebay.net/trackprogress, *accessed* January 2014.

Cooper, J.R., J.W. Gilliam, R.B. Daniels, and W.P. Robarge, 1987. Riparian Areas as Filters for Agricultural Sediment. Soil Science Society of America Journal 51:416-420, doi: 10.2136/sssaj1987.03615995005100020029x.

Daniels, R.B. and J.W. Gilliam, 1996. Sediment and Chemical Load Reduction by Grass and Riparian Filters. Soil Science Society of America Journal 60:246-251, doi: 10.2136/sssaj1996.03615995006000010037x.

Day, T.J., 1976. On the Precision of Salt Dilution Gauging. Journal of Hydrology 31:293-306, doi: 10.1016/0022-1694(76)90130-X.

Dillaha, T.A., 1987. Evaluating Nutrient and Sediment Losses from Agricultural Lands: Vegetative Filter Strips. CBP/TRS (USA).

Dillaha, T.A., R.B. Reneau, S. Mostaghimi, and D. Lee, 1989. Vegetative Filter Strips for Agricultural Nonpoint Source Pollution-Control. Transactions of the ASAE 32:513-519.

Dosskey, M.G., D.E. Eisenhauer, and M.J. Helmers, 2005. Establishing Conservation Buffers Using Precision Information. Journal of Soil and Water Conservation 60:349-354.

Dosskey, M.G., M.J. Helmers, D.E. Eisenhauer, T.G. Franti, and K.D. Hoagland, 2002. Assessment of Concentrated Flow through Riparian Buffers. Journal of Soil and Water Conservation 57:336-343.

Dosskey, M.G., Z. Qiu, M.J. Helmers, and D.E. Eisenhauer, 2011. Improved Indexes for Targeting Placement of Buffers of Hortonian Runoff. Journal of Soil and Water Conservation 66:362-372.

Dosskey, M.G., P. Vidon, N.P. Gurwick, C.J. Allan, T.P. Duval, and R. Lowrance, 2010. The Role of Riparian Vegetation in Protecting and Improving Chemical Water Quality in Streams. Journal of the American Water Resources Association 46:261-277, doi: 10.1111/j.1752-1688.2010.00419.x.

Fox, G.A., R. Muñoz-Carpena, and G.J. Sabbagh, 2010. Influence of Flow Concentration on Parameter Importance and Prediction Uncertainty of Pesticide Trapping by Vegetative Filter Strips. Journal of Hydrology 384:164-173, doi: 10.1016/j.jhydrol.2010.01.020.

Helmers, M.J., D.E. Eisenhauer, M.G. Dosskey, T.G. Franti, J.M. Brothers, and M.C. McCullough, 2005. Flow Pathways and Sediment Trapping in a Field-Scale Vegetative Filter. Transactions of the ASAE 48:955-968.

Hösl, R., P. Strauss, and T. Glade, 2012. Man-Made Linear Flow Paths at Catchment Scale: Identification, Factors and Consequences for the Efficiency of Vegetated Filter Strips. Landscape and Urban Planning 104:245-252, doi: 10.1016/j.landurbplan.2011.10.017.

Jenson, S.K. and J.O. Domingue, 1988. Extracting Topographic Structure from Digital Elevation Data for Geographic Information-System Analysis. Photogrammetric Engineering and Remote Sensing 54:1593-1600.

Kemp, W.M., W.R. Boynton, J.E. Adolf, D.F. Boesch, W.C. Boicourt, G. Brush, J.C. Cornwell, T.R. Fisher, P.M. Glibert, J.D. Hagy, L.W. Harding, E.D. Houde, D.G. Kimmel, W.D. Miller, R. Newell, M.R. Roman, E.M. Smith, and J.C. Stevenson, 2005. Eutrophication of Chesapeake Bay: Historical Trends and Ecological Interactions. Marine Ecology Progress Series 303:1-29, doi: 10.3354/meps303001.

Kleinman, P.J.A., A.N. Sharpley, R.W. McDowell, D.N. Flaten, A.R. Buda, L. Tao, L. Bergstrom, and Q. Zhu, 2011. Managing Agricultural Phosphorus for Water Quality Protection: Principles for Progress. Plant and Soil 349:169-182, doi: 10.1007/s11104-011-0832-9.

Knight, K.W., R.C. Schultz, C.M. Mabry, and T.M. Isenhart, 2010. Ability of Remnant Riparian Forests, with and without Grass Filters, to Buffer Concentrated Surface Runoff. Journal of the American Water Resources Association 46:311-322, doi: 10.1111/j.1752-1688.2010.00422.x.

Lowrance, R., L.S. Altier, J.D. Newbold, R.R. Schnabel, P.M. Groffman, J.M. Denver, D.L. Correll, J.W. Gilliam, J.L. Robinson, and R.B. Brinsfield, 1997. Water Quality Functions of Riparian Forest Buffers in Chesapeake Bay Watersheds. Environmental Management 21:687-712.

Lowrance, R., J.K. Sharpe, and J.M. Sheridan, 1986. Long-Term Sediment Deposition in the Riparian Zone of a Coastal Plain Watershed. Journal of Soil and Water Conservation 41:266-271.

Lowrance, R., R. Todd, J. Fail, J.H. Joseph, R.L. Ole, and L. Asmussen, 1984. Riparian Forests as Nutrient Filters in Agricultural Watersheds. BioScience 34:374-377, doi: 10.2307/1309729.

Mayer, P.M., S.K. Reynolds, M.D. McCutchen, and T.J. Canfield, 2007. Meta-Analysis of Nitrogen Removal in Riparian Buffers. Journal of Environmental Quality 36:1172, doi: 10.2134/jeq2006.0462.

National Research Council, 2011. Achieving Nutrient and Sediment Reduction Goals in the Chesapeake Bay: An Evaluation of Program Strategies and Implementation. The National Academies Press, Washington D.C., ISBN 9780309210799.

Officer, C.B., R.B. Biggs, J.L. Taft, L.E. Cronin, M.A. Tyler, and W.R. Boynton, 1984. Chesapeake Bay Anoxia: Origin, Development, and Significance. Science 223:22-27, doi: 10.1126/science.223.4631.22.

Pankau, R.C., J.E. Schoonover, K.W.J. Williard, and P.J. Edwards, 2011. Concentrated Flow Paths in Riparian Buffer Zones of Southern Illinois. Agroforestry Systems 84:191-205, doi: 10.1007/s10457-011-9457-5.

Peterjohn, W.T. and D.L. Correll, 1984. Nutrient Dynamics in an Agricultural Watershed: Observations on the Role of a Riparian Forest. Ecology 65:1466, doi: 10.2307/1939127.

Tomer, M.D., M.G. Dosskey, M.R. Burkart, D.E. James, M.J. Helmers, and D.E. Eisenhauer, 2009. Methods to Prioritize Placement of Riparian Buffers for Improved Water Quality. Agroforestry Systems 75:17-25, doi: 10.1007/s10457-008-9134-5.

Tomer, M.D., D.E. James, and T.M. Isenhart, 2003. Optimizing the Placement of Riparian Practices in a Watershed Using Terrain Analysis. Journal of Soil and Water Conservation 58:198-206.

USEPA (United States Environmental Protection Agency), 2010. Chesapeake Bay Total Maximum Daily Load for Nitrogen, Phosphorus and Sediment: Sources of Nutrients and Sediment to the Chesapeake Bay, Washington, D.C. http://www.epa.gov/reg3wapd/pdf/pdf_chesbay/FinalBayTMDL/CBayFinalTMDLExecSumSection1through3_final.pdf, *accessed* January 2015.

USGS (United States Geological Survey), 2014. About NED. SGS National Geospatial Program, Reston, Virginia. http://ned.usgs.gov/about.html, *accessed* January 2015.

Verstraeten, G., J. Poesen, K. Gillijns, and G. Govers, 2006. The Use of Riparian Vegetated Filter Strips to Reduce River Sediment Loads: An Overestimated Control Measure? Hydrological Processes 20:4259-4267, doi: 10.1002/hyp.6155.

Virginia General Assembly, 1989. 9VAC25-830-80: Resource Protection Areas. http://law.lis.virginia.gov/vacode, *accessed* January 2015.